Title: Testing for the effects of pre-season temperature and winter-chilling on land-surface phenology of coniferous and broadleaved forests in Central Europe

Authors: Cornelius Senf and Tobias Krueger

Affiliation: Integrative Research Institute on Transformation of Human-Environment Systems (IRI THESys), Humboldt-Universität zu Berlin, Unter den Linden 6, 10099 Berlin, Germany

Correspondence to: Cornelius Senf; E-Mail: corneliussenf@googlemail.com

Keywords: Phenology; Remote sensing; Climate change; Bayesian hierarchical modelling; Landsat

Abstract: Phenology is an important indicator of climate change impacts on vegetated ecosystems. Changes in leaf unfolding dates in response to changing temperatures have been well documented from in-situ phenological measurements across Central Europe. However, it is unclear whether those processes can be scaled to the landscape scale, which is important to accurately represent phenology in (global) vegetation models. Moderate resolution remote sensing time series, which measure land surface phenology instead of species specific phenophases, can help answering this question. We here test for the effect of pre-season temperature and winter-chilling on the inter-annual variation in start of season derived from Landsat time series for a forest landscape in southern Germany. The landscape is comprised of broadleaved and coniferous forests and thus typical for montane forest landscapes in Central Europe. We find strong evidence for average pre-season mean daily temperature driving inter-annual variation in start of season, with a -3.74 d $°C^{-1}$ earlier start of season for broadleaved forests and a -2.68 d $°C^{-1}$ earlier start of season for coniferous forests over the time period 1985 to 2015. This relationship, however, was modulated by the number of chilling days during winter, with a decreasing effect of pre-season temperature with decreasing number of chilling days. The inter-annual variation in start of season predicted from our model – i.e., calibrated solely from Landsat satellite time series – showed good agreement with in-situ observations of bud-break (Pearson's r = 0.79/RMSE = 4.88 d for broadleaved forests and r = 0.62/RMSE = 6.57 d for coniferous forests). We conclude that in-situ based processes are also detectable at the landscape-scale and that considering winter-chilling is important for accurately predicting phenology, which should be recognized in (global) vegetation models.

1. Introduction

Phenology is a key property of ecosystems (Forrest & Miller-Rushing, 2010). Due to its sensitivity to climate, phenology is also a valuable indicator of climate change (Cleland, Chuine, Menzel, Mooney, & Schwartz, 2007). Climate change effects on vegetation phenology have been documented in numerous experimental and observational studies, finding shifts in the start of the growing season for many plant species as a result of climate change (Cleland et al., 2007; Menzel et al., 2006; Parmesan & Yohe, 2003). Those changing phenological patterns have profound impacts on ecosystem functions, such as carbon uptake (Keenan et al., 2014). In order to better understand the impacts of changing phenology on ecosystem function, it is fundamental to monitor, model and ultimately predict vegetation phenological dynamics at varying spatial and temporal scales (Pau et al., 2011; Tang et al., 2016).

A key data source for monitoring and modeling phenological dynamics are in-situ phenological measurements. Those measurements are generally taken at the level of individuals (e.g., single trees or plants), and the resulting information is used to calibrate species-specific phenological models that predict phenological phases (e.g., leaf unfolding) based on a set of aggregated meteorological variables (Basler, 2016; Chuine, 2000; Hufkens, Basler, Milliman, Melaas, & Richardson, 2018). However, such species-specific models are often difficult to regionalise to the landscape or ecosystem scale (Y. Fu, Zhang, Dong, & Yuan, 2014; Richardson et al., 2012; Tang et al., 2016), particularly if the exact species or community composition are unknown (Jeremy I. Fisher, Richardson, & Mustard, 2007; Liang & Schwartz, 2009). Further, calibrating species-specific models across large geographic extents is challenging, as in-situ phenological observations are lacking in many regions worldwide, or are difficult to compare due to varying measurement protocols and/or target species (Fitchett, Grab, & Thompson, 2015). An improved understand of phenological dynamics at the landscape and ecosystem scale is, however, required for further developing

the representation of phenology in global vegetation models (Richardson et al., 2012; Yang, Mustard, Tang, & Xu, 2012).

Remote sensing, which measures so-called land surface phenology and thus delivers an integrated view on phenology independent of individual species (Morisette et al., 2009), might overcome limitations of field-based phenological data. Classical approaches tracking phenology from remote sensing data made use of the synoptic view of the Advanced Very High Resolution Radiometer (AVHRR) sensor family (M. A. White et al., 2009). AVHRR, however, has a spatial resolution that is too coarse (1 km) to infer phenological dynamics in spatially heterogeneous landscapes. The MODerate Imaging Spectroradiometer (MODIS), which has a higher spatial resolution of 250 m, might improve the estimation of spatial drivers (Friedl et al., 2014), yet its limited temporal depth (starting in 2001) makes it difficult to infer temporal trends in phenological dynamics. Dense Landsat time series were recently suggested to overcome the limitations of MODIS and AVHRR in monitoring vegetation phenology (J. I. Fisher & Mustard, 2007; J. I. Fisher, Mustard, & Vadeboncoeur, 2006; Melaas, Friedl, & Zhu, 2013; Melaas, Sulla-Menashe, & Friedl, 2018; Nijland, Bolton, Coops, & Stenhouse, 2016; Senf, Pflugmacher, Heurich, & Krueger, 2017), since they have a spatial resolution of 30 m and cover a time-span of more than 30 years (from 1984 onwards). Landsat time series might thus be well suited to characterize vegetation phenology at the landscape scale, and thus gain additional insights supporting field-based phenological studies.

For Central Europe, a substantial shift in leaf unfolding was identified over the past four decades (Menzel et al., 2006). It was hypothesized that warmer spring temperatures caused by climate change are the main driver explaining this observation. Yet, more recent research highlights the importance of winter chilling for phenological dynamics (Y. H. Fu, Piao, et al., 2015; Y. H. Fu, Zhao, et al., 2015; Laube et al., 2014). In particular, the effect of warmer spring temperatures on leaf unfolding might be compensated by reduced winter-chilling with increasing winter temperatures. While the modulating effect of winter chilling is

increasingly well understood based on lab experiments and field studies, it is unknown whether it also reproduces at the landscape scale, that is, whether similar effects can be found for land surface phenology derived from satellite time series.

We here test for the interacting effects of pre-season temperature and winter-chilling on the inter-annual variation in start of season derived from Landsat time series. Our hypothesis was that while warmer pre-season temperatures would lead to earlier start of seasons, the effect will be modulated by the number of chilling days during winter. For testing this hypothesis, we integrate Landsat time series and meteorological observations into a combined phenological model. We calibrate the model for a landscape in southern Germany, comprised of broadleaved and coniferous forests, thus representing typical forest types in Central European (sub-) montane landscapes. We finally compare predictions from our model to in-situ phenological observations of leaf unfolding, determining whether pre-season temperature and winter-chilling effects identified from land surface phenology reproduce field-based observations of leaf-unfolding.

2. Data and methods

2.1 Study landscape

The study landscape is located in the Bavarian Forest National park, with moderate topography ranging from approximately 300 to 1,800 meters in elevation (Figure 1). The ecosystem is characterized by mountain beech forests with *Fagus sylvatica* (European beech) being the leading species. Other broad-leaved tree species include *Acer pseudoplatanus* (Sycamore maple) or *Quercus robur* (English oak), but *F. sylvatica* is by far the most abundant. The higher elevation areas of the ecosystem, in turn, are covered by mountain spruce forests, consisting mainly of *Picea abies* (Norway spruce), with some *Abeis alba* (European silver fir) intermixed.

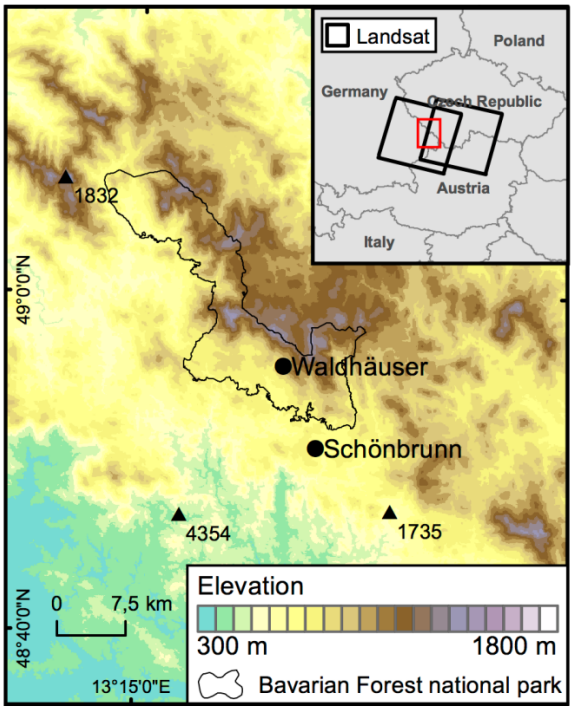

Figure 1: Study landscape with national park boundaries, the three meteorological stations (triangles), and the two in-situ phenological observation sites (points) from the International Phenological Gardens of Europe network.

2.2 Landsat data

Landsat has been used to create wall-to-wall maps of phenological parameters (e.g., start of season), which were subsequently used to summarize the inter-annual variability in each parameter for a specific ecosystem or region (Melaas et al., 2013; Nijland et al., 2016). However, creating wall-to-wall maps is computationally intensive and might be too cumbersome if one is primarily interested in estimating the temporal dynamics of phenology for a certain landscape or ecosystem. Alternatively, a sample-based approach can be used, where only a sample of the Landsat time series is used to estimate the temporal dynamics in phenological metrics (Melaas et al., 2018; Senf et al., 2017). We identified suitable sampling locations for both broadleaved forests (i.e., mountain beech forests) and coniferous forests (i.e., mountain spruce forests) using an existing land cover map generated by National Park authorities from aerial imagery. To exclude young and/or disturbed forests we only sampled mature stands, that is, stands with a minimum age of 60 years. The sample size was set to n =

250, but we also tested alternative sample sizes with no substantial differences found (data not shown).

We created cloud-, snow-, and shadow-free Enhanced Vegetation Index (EVI) time series for each sample location using all data from the Landsat archive, accessed via the Google Earth Engine (Gorelick et al., 2017). We preferred EVI over other vegetation indices as it has been shown to allow better estimation of key phenological dates from remote sensing data (Klosterman et al., 2014). Finally, as we were primarily interested in spring phenology, we separated the time series into spring/summer and autumn/winter observations. We followed a method suggested by Melaas et al. (2013), which excludes all observations before day of year 80 (winter observations) and then uses an iterative algorithm identifying the transition from summer to autumn. In essence, the algorithm fits a linear model to a running window of 21 observations and identifies the day of year with the first negative slope as the summer-autumn transition date. We dropped all autumn/winter observations from further analysis.

2.3 Meteorological data

We used meteorological data to created annual estimates of pre-season temperature and winter chilling for the study landscape. Pre-season temperature (T_{pre}) was defined as the average mean daily temperature T_{mean} in the months April and May, being the approximate months of vegetation green-up in our study region (Senf et al., 2017). Winter chilling (D_{chil}) was defined as the number of days with $0 < T_{mean} \leq 5\ ^\circ C$ as suggested by previous studies (Y. H. Fu, Zhao, et al., 2015). Both variables were averaged from three meteorological stations operated by the German Weather Service (station-ids: 1735, 1832, 4354; Figure 1; ftp://ftp-cdc.dwd.de/pub/CDC/observations_germany/climate/daily/kl/historical/). We restricted the time-series to our study period (1985 – 2015) and z-transformed the data to represent anomalies in units of standard deviation.

2.4 Landsat phenological model

To estimate average phenological parameters for each pixel sampled, all available EVI observations are sorted by observation day of year t, independent of the year of observation (see Figure 2). Following previous research (Elmore, Guinn, Minsley, & Richardson, 2012; K. White, Pontius, & Schaberg, 2014), we model this average phenological curve by a logistic function with four parameters and normally distributed errors (see Figure 2 and Table 1):

$$EVI_i = \beta_{1[i]} + \frac{\beta_{2[i]}}{\left(1 + e^{-\beta_{3[i]} * (t - \beta_{4[i]})}\right)} + \varepsilon_i$$
$$\varepsilon_i \sim N(0, \sigma^2) \quad (1)$$

The parameters ($\boldsymbol{\beta}_i$) of the logistic function were modelled as a multivariate normal distribution, thus allowing for correlation between them. We re-parameterized the multivariate normal distribution to improve model convergence following recommendations in Senf et al. (2017).

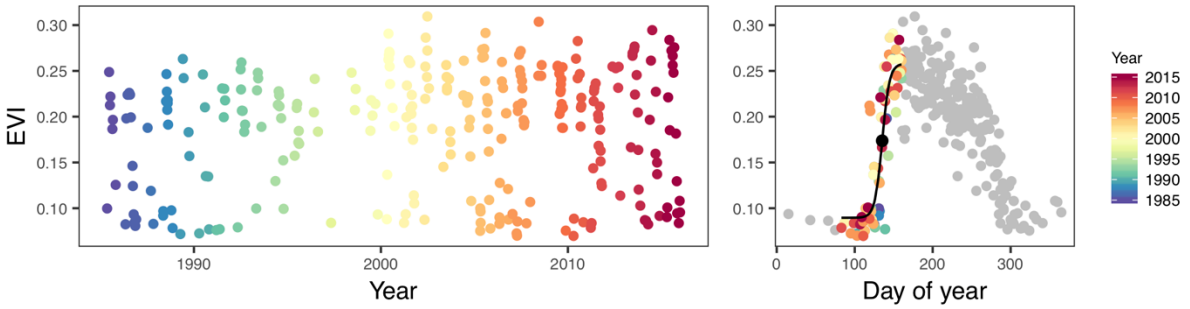

Figure 2: Example pixel time series showing the annual observations (left panel) and the pooled time series (right panel). Shown here is the Enhanced Vegetation Index (EVI). The pooled time series is truncated to spring and summer observations as described in Section 2.3, and only those observations are colored. A phenological model as described in Section 2.4 was fit to the data. The black dot represents the start of season estimated from the model.

Table 1: Phenological parameters of the model.

Parameters $\boldsymbol{\beta}_i$	Name	Description

$\beta_{1[i]}$	Minimum	The minimum spectral value.
$\beta_{2[i]}$	Magnitude	The magnitude of spectral change during the year.
$\beta_{3[i]}$	Change rate	The change rate in the inflection point.
$\beta_{4[i]}$	Start of season	The day of year of the inflection point.

To account for temporal variation in the model parameters $\boldsymbol{\beta}_i$ among years j, we follow Senf et al. (2017) and replace $\boldsymbol{\beta}_i$ by a hierarchical formulation: $\boldsymbol{\beta'}_{ij} = \boldsymbol{\beta}_i + \boldsymbol{\phi}_j$, allowing them to simultaneously vary in space and time. Thus, the model estimates average phenological parameters for each pixel, and simultaneously estimates how each parameters varies – on average – over time. While the variability in the minimum, maximum and change rate is assumed to be purely random (i.e., expressed by a multivariate normal distribution centered on zero), we specifically model the mean temporal variation in the start of season by a linear combination of pre-season temperature and winter-chilling (and their interaction): $\phi_{4[j]} \sim N(\rho_1 * T_{pre} + \rho_2 * D_{chil} + \rho_3 * T_{pre} * D_{chil}, \sigma_\rho^2)$. Hence, the model estimates the direction and strength of influence of pre-season temperature, winter chilling and their interaction on the inter-annual variability in the start of season.

2.5 Parameter estimation

Full Bayesian inference for each model parameter was made by sampling the joint posterior distribution using Markov Chain Monte Carlo (MCMC) methods implemented in the free software Stan (Carpenter et al., 2017). To sample joint posterior distributions, we needed to assign prior distributions to each parameter. We used weakly-informative, penalizing priors, which put most probability mass on values around zero. There must thus be high evidence in the data to estimate a posterior effect that is substantially different from zero (similar to lasso-regression). Further, we centered priors of the four parameters of the logistic function to their approximate location by averaging over the estimates of 10 non-linear least square fits with standard settings. While this step is not necessary to run the model, it helps making the model

converge faster and is thus similar to setting initial starting values in other (frequentist) iterative fitting routines.

The joint posterior distributions were finally sampled using four chains à 4,000 iterations, of which 2,000 were later dropped as warm-up iterations. Convergence of chains was tested by comparing the between- and within-chain variance using the $\hat{R}$ statistic described in Gelman, Carlin, Stern, and Rubin (2014). In essence, the $\hat{R}$ statistic compares the variance within each chain to the variance between chains, with values approaching 1.00 if chains converge to a similar solution. While modern MCMC samplers greatly improved in terms of speed, sampling might still take a long time with very large samples of pixels. To overcome this inherent limitation of spatial Bayesian statistics, we implemented an ensemble pixel sampling strategy that draws m samples of n pixels, and later average over the m joint posterior probability distributions of each model parameter. The associated cost of greater imprecision of parameter estimates due to the relatively small pixel sample size and the averaging of the posterior distributions was mitigated by a sufficient number of ensemble members (see Figure S1).

We finally tested the fit of the ensemble model by means of posterior predictive checking. Posterior predictive checking generates replicated data drawn randomly under the model, which can then be compared to the observed data (Gelman et al., 2014). If the model fits the data well, there should be no systematic differences between the replicated data and the observed vegetation index time series.

2.6 Comparison to in-situ measurements

After sampling the joint posterior distribution, we compared the predicted inter-annual variability in the start of season against in-situ observations of leaf unfolding recorded for three *F. sylvatica* trees and three *P. abies* trees at two phenological gardens within and in close proximity to the National Park, respectively (see Figure 1). The phenological

218 observations were acquired from the International Phenological Gardens of Europe network
219 (stations: Waldhäuser and Schönbrunn; Figure 1; http://ipg.hu-berlin.de/).

220 **3. Results**

221 ***3.1 Model evaluation***

222 All models in the ensemble showed good convergence with $\hat{R}$ smaller 1.01 for 99% of the
223 model parameters. Posterior predictive checks indicated no systematic deviation between
224 simulated and raw values (Figure S2), and 96% of the raw values were within the 95%
225 credible interval of the posterior simulations. Hence, there was little evidence to assume a
226 substantial mismatch between model and data.

227 ***3.2 Inter-annual variability in start of season***

228 We identified substantial inter-annual variability in the start of season for broadleaved and
229 coniferous forests (Figure 3), with an average change of -0.3 d yr^{-1} for broadleaved and of -
230 0.4 d yr^{-1} for coniferous forests. This result indicates that the start of season was
231 approximately 9 and 12 days earlier in 2015, compared to 1985, for broadleaved and
232 coniferous forests, respectively. There were also some very late years (e.g., 1991) and some
233 very early years (e.g., 2007 and 2009) identifiable for both broadleaved and coniferous
234 forests, with overall very similar inter-annual variability for both forest types.

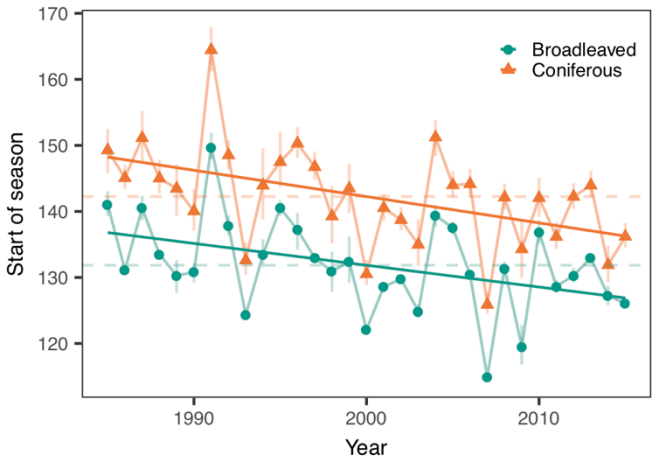

235

236 **Figure 3:** Inter-annual variability in start of season estimated from Landsat time series for
237 two forest types. Dots represent the median of the posterior distribution and error-bars extent

from the 2.5% to the 97.5% quantile of the posterior (95% credible interval). The dashed horizontal lines indicate the long-term average, whereas the solid lines indicate the trend line (OLS-estimate of the posterior medians).

3.3 Driver analysis

The driver analysis revealed that the inter-annual variability in the start of season is highly sensitive to pre-season temperature (Figure 4), with a -3.7 d $°C^{-1}$ earlier start of season for broadleaved and a -2.7 d $°C^{-1}$ earlier start of season for coniferous forests, respectively. The effect of pre-season temperature on inter-annual variability in start of season was, however, modulated by the total number of chilling days in the preceding winter (Figure 4), with a decreasing effect of pre-season temperature on inter-annual variability in the start of season with a decreasing number of chilling days (Figure 5). Hence, the advance in spring phenology following a warmer than average spring were less pronounced when the preceding winter had a below-average number of chilling days.

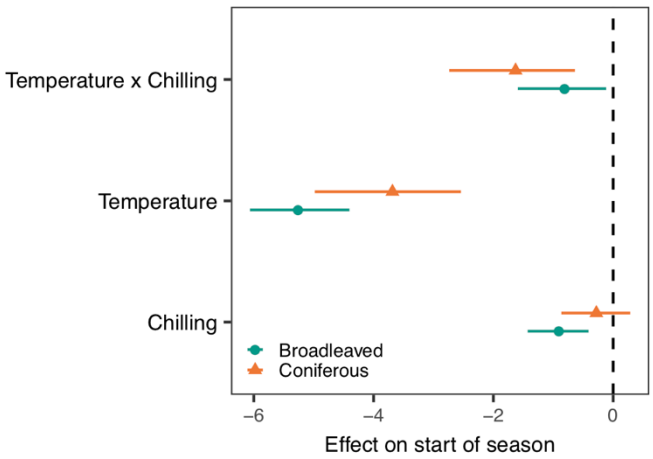

Figure 4: Effects of pre-season temperature and winter-chilling on start of season. All variables are z-transformed and effects are thus on the standard deviation scale. Dots represent the median of the posterior distribution and error-bars extent from the 2.5% to the 97.5% quantile of the posterior (95% credible interval).

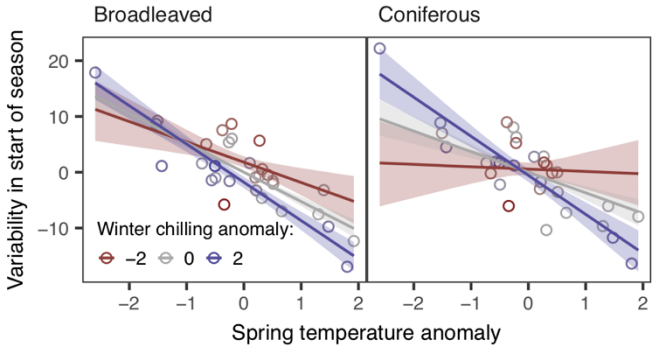

Figure 5: Variability in start of season with changing pre-season temperature and changing number of winter-chilling days as estimated from the model.

3.4 Comparison to in-situ measurements

Comparing predictions from the model (i.e., based on the regression relationship shown in Figure 5) to in-situ observations of bud-break (Figure 6), we found strong agreement for broadleaved forests (Pearson's r = 0.79 [0.74 – 0.80] and RMSE = 4.88 [4.60 – 5.21] days) and moderate agreement for coniferous forests (Pearson's r = 0.69 [0.63 – 0.75] and RMSE = 6.57 [6.00 – 7.13] days). Hence, our model – based only on pre-season temperature and winter chilling and calibrated solely from Landsat time series – was able to predict the general inter-annual variability in spring phenology as recorded in in-situ measurements.

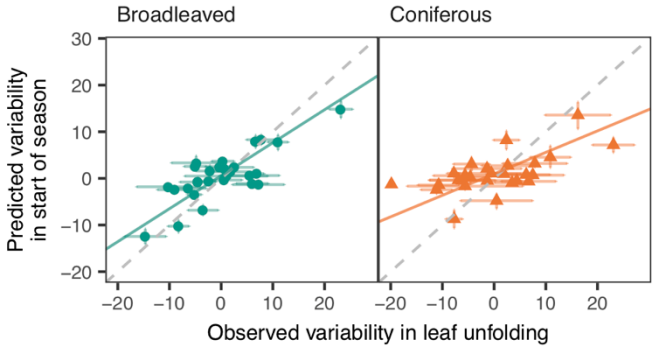

Figure 6: Comparing the inter-annual variability in start of season predicted from our model to in-situ observations of leaf unfolding derived from two phenological gardens in and around the national park (see Figure 1). Dots represent the median of the posterior (prediction; y-axis) and the arithmetic mean (leaf unfolding; x-axis). Uncertainty in the prediction is expressed by

the 95% credible interval, whereas error-bars for the leaf unfolding represent 95% confidence intervals.

4. Discussion

We here used dense Landsat time series to test for the interacting effects of pre-season temperature and winter-chilling on the inter-annual variation in start of season. We did so by explicitly integrating Landsat time series with meteorological observations; that is, instead of creating phenological products from remote sensing data that are subsequently used in analysis, we here calibrated phenological models directly from the millions of spectral observations available through the Landsat archive. The advantage is a reduced number of, and redundancy in, processing steps; as well as a better propagation of uncertainty, which is otherwise largely neglected in remotely sensed phenological studies.

Our model – calibrated solely from Landsat observations – was capable of predicting inter-annual variability in leaf-unfolding observed in-situ, despite the relatively simple model structure. This finding reinforces previous studies showing that more complex models do not necessarily lead to better predictions (Basler, 2016; Yang et al., 2012). In fact, RMSE values obtained by our model are in a similar range or even lower than comparable or more complex phenological models (Basler, 2016; Hufkens et al., 2018). Further, as our model is calibrated on land surface phenology (Morisette et al., 2009), it might better represent the landscape- and ecosystem-scale drivers of phenology than models based on species-specific in-situ observations (Liang & Schwartz, 2009). This is mainly due to a more aggregated view going beyond individual species and species differences (Jeremy I. Fisher et al., 2007). This difference might be particularly important for calibrating phenological models used in global vegetation models (Richardson et al., 2012; Yang et al., 2012).

The effects of pre-season temperature and winter-chilling on inter-annual variability in start of season identified in this study largely corroborate the current literature based on in-situ observations and lab experiments (Y. H. Fu, Piao, et al., 2015; Y. H. Fu, Zhao, et al.,

2015; Laube et al., 2014). Thus, recent insights on the importance of winter-chilling for phenological dynamics also reproduce at the landscape scale, highlighting the need for including those processes into (global) vegetation models. From an ecosystem-scale perspective, this might indicate that warming-related reductions in chilling days might slow down recent observed changes in spring phenology, with cascading effects on other ecosystem processes thus as carbon uptake. Yet, the exact processes are still elusive, and additional drivers such as precipitation or the previous year's phenology are discussed in the current literature (Y. H. Fu, Piao, et al., 2015; Y. S. Fu et al., 2014). Our model – in conjunction with global long-term satellite records from the Landsat archive – can be extended to include those drivers and thus offers great potential for understanding phenological responses under climate change in more detail.

5. Conclusion

We here used dense Landsat time series to show the interacting effects of pre-season temperature and winter-chilling on the inter-annual variation in start of season. We thus found additional evidence for the combined effect of temperature forcing and winter chilling in predicting the start of season, but also showing that the relationship holds true at the landscape scale. Hence, our research suggests that ecosystem models incorporating phenology should recognize the importance of winter chilling, especially under climate change scenarios. Remote sensing – and in particular Landsat remote sensing – might help calibrating those models, as we here showed Landsat-based models can reproduce field-based estimates, which are rare in many regions worldwide.

Acknowledgements

Cornelius Senf and Tobias Krueger are both funded through IRI THESys by the German Excellence Initiative. We thank Prof. Dr. Frank-M. Chmielewski of Humboldt-Universität zu Berlin for access to the phenological observations. We also thank Marius Derenthal for help with code implementation in the Google Earth Engine.

Data and code accessibility

All data and code used in this publication are available for review at https://github.com/corneliussenf/phenoBayes_drivers and will be archived using https://zenodo.org/ after the paper has been accepted for publication.

References

Basler, D. (2016). Evaluating phenological models for the prediction of leaf-out dates in six temperate tree species across central Europe. *Agricultural and Forest Meteorology, 217*, 10-21. doi:10.1016/j.agrformet.2015.11.007

Carpenter, B., Gelman, A., Hoffman, M. D., Lee, D., Goodrich, B., Betancourt, M., . . . Riddell, A. (2017). Stan: A Probabilistic Programming Language. *Journal of Statistical Software, 76*(1), 1-32. doi:10.18637/jss.v076.i01

Chuine, I. (2000). A unified model for budburst of trees. *J Theor Biol, 207*(3), 337-347. doi:10.1006/jtbi.2000.2178

Cleland, E. E., Chuine, I., Menzel, A., Mooney, H. A., & Schwartz, M. D. (2007). Shifting plant phenology in response to global change. *Trends Ecol Evol, 22*(7), 357-365. doi:10.1016/j.tree.2007.04.003

Elmore, A. J., Guinn, S. M., Minsley, B. J., & Richardson, A. D. (2012). Landscape controls on the timing of spring, autumn, and growing season length in mid-Atlantic forests. *Global Change Biology, 18*(2), 656-674. doi:10.1111/j.1365-2486.2011.02521.x

Fisher, J. I., & Mustard, J. F. (2007). Cross-scalar satellite phenology from ground, Landsat, and MODIS data. *Remote Sensing of Environment, 109*(3), 261-273. doi:10.1016/j.rse.2007.01.004

Fisher, J. I., Mustard, J. F., & Vadeboncoeur, M. A. (2006). Green leaf phenology at Landsat resolution: Scaling from the field to the satellite. *Remote Sensing of Environment, 100*(2), 265-279. doi:10.1016/j.rse.2005.10.022

Fisher, J. I., Richardson, A. D., & Mustard, J. F. (2007). Phenology model from surface meteorology does not capture satellite-based greenup estimations. *Global Change Biology, 13*(3), 707-721. doi:10.1111/j.1365-2486.2006.01311.x

Fitchett, J. M., Grab, S. W., & Thompson, D. I. (2015). Plant phenology and climate change: Progress in methodological approaches and application. *Progress in Physical Geography, 39*(4), 460-482. doi:10.1177/0309133315578940

Forrest, J., & Miller-Rushing, A. J. (2010). Toward a synthetic understanding of the role of phenology in ecology and evolution. *Philos Trans R Soc Lond B Biol Sci, 365*(1555), 3101-3112. doi:10.1098/rstb.2010.0145

Friedl, M. A., Gray, J. M., Melaas, E. K., Richardson, A. D., Hufkens, K., Keenan, T. F., . . . O'Keefe, J. (2014). A tale of two springs: using recent climate anomalies to characterize the sensitivity of temperate forest phenology to climate change. *Environmental Research Letters, 9*(5). doi:Artn 054006
10.1088/1748-9326/9/5/054006

Fu, Y., Zhang, H., Dong, W., & Yuan, W. (2014). Comparison of phenology models for predicting the onset of growing season over the Northern Hemisphere. *PLoS One, 9*(10), e109544. doi:10.1371/journal.pone.0109544

Fu, Y. H., Piao, S., Vitasse, Y., Zhao, H., De Boeck, H. J., Liu, Q., . . . Janssens, I. A. (2015). Increased heat requirement for leaf flushing in temperate woody species over 1980-2012: effects of chilling, precipitation and insolation. *Glob Chang Biol, 21*(7), 2687-2697. doi:10.1111/gcb.12863

Fu, Y. H., Zhao, H., Piao, S., Peaucelle, M., Peng, S., Zhou, G., . . . Janssens, I. A. (2015). Declining global warming effects on the phenology of spring leaf unfolding. *Nature, 526*(7571), 104-107. doi:10.1038/nature15402

Fu, Y. S., Campioli, M., Vitasse, Y., De Boeck, H. J., Van den Berge, J., AbdElgawad, H., . . . Janssens, I. A. (2014). Variation in leaf flushing date influences autumnal senescence and next year's flushing date in two temperate tree species. *Proc Natl Acad Sci U S A, 111*(20), 7355-7360. doi:10.1073/pnas.1321727111

Gelman, A., Carlin, J. B., Stern, H. S., & Rubin, D. B. (2014). *Bayesian data analysis* (Vol. 2): Chapman & Hall/CRC Boca Raton, FL, USA.

Gorelick, N., Hancher, M., Dixon, M., Ilyushchenko, S., Thau, D., & Moore, R. (2017). Google Earth Engine: Planetary-scale geospatial analysis for everyone. *Remote Sensing of Environment, 202*, 18-27. doi:10.1016/j.rse.2017.06.031

Hufkens, K., Basler, D., Milliman, T., Melaas, E. K., & Richardson, A. D. (2018). An integrated phenology modelling framework in R. *Methods in Ecology and Evolution, 9*(5), 1276-1285. doi:10.1111/2041-210x.12970

Keenan, T. F., Gray, J., Friedl, M. A., Toomey, M., Bohrer, G., Hollinger, D. Y., . . . Richardson, A. D. (2014). Net carbon uptake has increased through warming-induced changes in temperate forest phenology. *Nature Climate Change, 4*(7), 598-604. doi:10.1038/Nclimate2253

Klosterman, S. T., Hufkens, K., Gray, J. M., Melaas, E., Sonnentag, O., Lavine, I., . . . Richardson, A. D. (2014). Evaluating remote sensing of deciduous forest phenology at multiple spatial scales using PhenoCam imagery. *Biogeosciences, 11*(16), 4305-4320. doi:10.5194/bg-11-4305-2014

Laube, J., Sparks, T. H., Estrella, N., Hofler, J., Ankerst, D. P., & Menzel, A. (2014). Chilling outweighs photoperiod in preventing precocious spring development. *Glob Chang Biol, 20*(1), 170-182. doi:10.1111/gcb.12360

Liang, L., & Schwartz, M. D. (2009). Landscape phenology: an integrative approach to seasonal vegetation dynamics. *Landscape Ecology, 24*(4), 465-472. doi:10.1007/s10980-009-9328-x

Melaas, E. K., Friedl, M. A., & Zhu, Z. (2013). Detecting interannual variation in deciduous broadleaf forest phenology using Landsat TM/ETM plus data. *Remote Sensing of Environment, 132*, 176-185. doi:10.1016/j.rse.2013.01.011

Melaas, E. K., Sulla-Menashe, D., & Friedl, M. A. (2018). Multidecadal Changes and Interannual Variation in Springtime Phenology of North American Temperate and Boreal Deciduous Forests. *Geophysical Research Letters, 45*(6), 2679-2687. doi:10.1002/2017gl076933

Menzel, A., Sparks, T. H., Estrella, N., Koch, E., Aasa, A., Ahas, R., . . . Zust, A. (2006). European phenological response to climate change matches the warming pattern. *Global Change Biology, 12*(10), 1969-1976. doi:10.1111/j.1365-2486.2006.01193.x

Morisette, J. T., Richardson, A. D., Knapp, A. K., Fisher, J. I., Graham, E. A., Abatzoglou, J., . . . Liang, L. (2009). Tracking the rhythm of the seasons in the face of global change: phenological research in the 21st century. *Frontiers in Ecology and the Environment, 7*(5), 253-260. doi:10.1890/070217

Nijland, W., Bolton, D. K., Coops, N. C., & Stenhouse, G. (2016). Imaging phenology; scaling from camera plots to landscapes. *Remote Sensing of Environment, 177*, 13-20. doi:10.1016/j.rse.2016.02.018

Parmesan, C., & Yohe, G. (2003). A globally coherent fingerprint of climate change impacts across natural systems. *Nature, 421*(6918), 37-42. doi:10.1038/nature01286

Pau, S., Wolkovich, E. M., Cook, B. I., Davies, T. J., Kraft, N. J. B., Bolmgren, K., . . . Cleland, E. E. (2011). Predicting phenology by integrating ecology, evolution and climate science. *Global Change Biology, 17*(12), 3633-3643. doi:10.1111/j.1365-2486.2011.02515.x

Richardson, A. D., Anderson, R. S., Arain, M. A., Barr, A. G., Bohrer, G., Chen, G. S., . . . Xue, Y. K. (2012). Terrestrial biosphere models need better representation of vegetation phenology: results from the North American Carbon Program Site Synthesis. *Global Change Biology, 18*(2), 566-584. doi:10.1111/j.1365-2486.2011.02562.x

Senf, C., Pflugmacher, D., Heurich, M., & Krueger, T. (2017). A Bayesian hierarchical model for estimating spatial and temporal variation in vegetation phenology from Landsat time series. *Remote Sensing of Environment, 194*, 155-160. doi:10.1016/j.rse.2017.03.020

Tang, J. W., Korner, C., Muraoka, H., Piao, S. L., Shen, M. G., Thackeray, S. J., & Yang, X. (2016). Emerging opportunities and challenges in phenology: a review. *Ecosphere, 7*(8), e01436-n/a. doi:ARTN e01436 10.1002/ecs2.1436

White, K., Pontius, J., & Schaberg, P. (2014). Remote sensing of spring phenology in northeastern forests: A comparison of methods, field metrics and sources of uncertainty. *Remote Sensing of Environment, 148*, 97-107. doi:10.1016/j.rse.2014.03.017

White, M. A., de Beurs, K. M., Didan, K., Inouye, D. W., Richardson, A. D., Jensen, O. P., . . . Lauenroth, W. K. (2009). Intercomparison, interpretation, and assessment of spring phenology in North America estimated from remote sensing for 1982-2006. *Global Change Biology, 15*(10), 2335-2359. doi:10.1111/j.1365-2486.2009.01910.x

Yang, X., Mustard, J. F., Tang, J. W., & Xu, H. (2012). Regional-scale phenology modeling based on meteorological records and remote sensing observations. *Journal of Geophysical Research-Biogeosciences, 117*(G3), n/a-n/a. doi:Artn G03029 10.1029/2012jg001977